Canadian Chemical Transactions

ISSN 2291-6458 (Print), ISSN 2291-6466 (Online)
Year 2013 | Volume 1 | Issue 3 | Page 215-237

Research Article

Quantum-chemical Modeling of the Relationships between Molecular Structure and *In Vitro* Multi-Step, Multimechanistic Drug Effects. HIV-1 Replication Inhibition and Inhibition of Cell Proliferation as Examples.

Juan S. Gómez-Jeria* **and Marcelo Flores-Catalán**

Quantum Pharmacology Unit, Department of Chemistry, Faculty of Sciences, University of Chile, P. O. Box 653, Santiago, Chile

**Corresponding Author, Email: facien03@uchile.cl Phone: +56-2-2978-7371, Fax: +56-2-2271-3888.*

Received: *September 13, 2013* ***Revised:*** *September 29, 2013* ***Accepted:*** *September 30, 2013* ***Published:*** *October 1, 2013*

Abstract: The general hypothesis that any *in vitro* or *in vivo* biological activity can be explained only in terms of local atomic reactivity indices has been proposed and tested for the inhibition of HIV-1 WT replication by some phenylaminopyridine derivatives and the inhibition of cell growth by several 1-azabenzanthrone derivatives. In all of them good structure-activity relationships have been obtained and some requirements for potent biological activity have been suggested. For the cases tested here the common skeleton hypothesis works well. As this hypothesis has a logical conceptual basis but does not yet have a formal general mathematical background, it cannot be generalized and must be tested case by case. This methodology gives an account of the whole process and, in the case of multi-step processes, is unable to relate the different reactivity indices appearing in the SAR equations to any particular step.

Keywords: Local atomic reactivity indices, DFT calculations, QSAR, SAR, HIV-1 replication, cell growth inhibition.

1. INTRODUCTION

During the last three decades we have developed a formal method [1] to correlate *in vitro* receptor binding affinity constants with the electronic structure and substituent orientational parameters of drug molecules [2-16]. A formal or non-empirical method is based on the following philosophy: it begins by proposing a model to explain a given biological activity. Next, by applying one or several physically-based approximations the assumptions of the model are translated into algebraic statements, deriving naturally one or more equations showing the expected relationships. A system of linear equations can be algebraically solved if at least the number of equations is the same than the number of variables. As this is not generally the case statistics is used, *not to see whether there is a structure-activity relationship, but to find the best one.*

ISSN 2291-6458 (Print), ISSN 2291-6466 (Online)
Year 2013 | Volume 1 | Issue 3 | Page 215-237

In our case the historical development of the model used here started with the work of Agin *et al.* during the 1960s [17], was continued by Cammarata [18-20], crystallized in the work of Peradejordi [21] and was extended by one of us. Over this period very many evaluations of pharmacological activity have been reported such as, for example, the inhibition of the appearance of macroscopic changes in biological systems (cytopathic effects and cell growth inhibition are good examples). Many of these *in vitro* effects are the ultimate result of two or more unidentified or unsatisfactorily known processes. This is a very important field of research that has not been explored by Quantum Pharmacology (QP) until recent times. Formal QP uses information coming only from quantum chemical calculations. The problem can be stated in a general form as: *what are the modifications that must be introduced into a formal model designed for in vitro drug-receptor interactions to allow us to study complex in vitro or in vivo processes?*

In this paper, and using such a model together with a generalization of several theoretical results obtained during the 1965-1975 decade, we demonstrate that the construction of this kind of structure-activity models is possible. We show the usefulness of our new model by presenting and analyzing structure-activity relationship results for the inhibition of HIV-1 WT replication by some phenylaminopyridine (PAP) derivatives [22] and for the inhibition of cell growth by several 1-azabenzanthrone derivatives [23]. Recently a series of compounds based on a 4-phenyl-2-phenylaminopyridine scaffold that are potent and selective inhibitors of Traf2- and Nck-interacting kinase activity have been described [24]. Benzanthrone is a basic substance with fluorescent and luminescent properties and it is used as an intermediate for anthraquinone-based dyes [25-30]. 3-Nitrobenzanthrone is a powerful mutagenic environmental contaminant.

2. THEORETICAL BACKGROUND

2.1. The model

We present below the formal model that correlates the drug-receptor affinity constant with the electronic and molecular structure of bioactive molecules. This model has shown, beyond all rational doubt, that it can shed light on the detailed structure of the drug-receptor interaction, that it has predictive capacity [5, 6, 31] and is even able to detect erroneous experimental data [32]. The last paper not belonging to our group, and using the model we are using here, was published in 1979 [33]. The reader should take care to distinguish it very clearly from the purely statistics-backed methodologies.

Let us consider the state of thermodynamic equilibrium, and a 1:l stoichiometry in the formation of the drug-receptor complex [3]:

$$D_i + R \rightleftarrows D_iR \qquad (1)$$

where D_i is the drug, R is the receptor, and D_iR is the drug-receptor complex. According to statistical thermodynamics the equilibrium constant, K_i, is written as:

$$K_i = \frac{Q_{D_iR}}{Q_{D_i} Q_R} \exp(-\Delta\varepsilon_0^i / kT) \qquad (2)$$

where $\Delta\varepsilon_0^i$ is the difference between the ground-state energy of D_iR and the energies of the ground states of D_i and R:

$$\Delta\varepsilon_0^i = \varepsilon_{D_iR} - (\varepsilon_{D_i} + \varepsilon_R) \qquad (3)$$

and the Q's are the total partition functions (PF) measured from the ground state (in solution). T and k are the temperature and the Boltzmann constant, respectively. Using well-grounded simplifications we may write Eq. 2 as [3]:

ISSN 2291-6458 (Print), ISSN 2291-6466 (Online)
Year 2013 | Volume 1 | Issue 3 | Page 215-237

$$\log K_i = a + bM_{D_i} + c\log\left[\sigma_{D_i}/(ABC)^{1/2}\right] + d\Delta\varepsilon_i \qquad (4)$$

where a, b, c and d are constants, *M* is the drug's mass, σ its symmetry number and *ABC* the product of the drug's moments of inertia about the three principal axes of rotation. The interaction energy, $\Delta\varepsilon_i$, cannot be determined directly, either due to the dimension of the receptor or to the lack of information about its detailed molecular structure. However, as we are dealing with a weak drug-receptor interaction, we can utilize Perturbation Theory in the Klopman-Hudson form to calculate $\Delta\varepsilon_i$ approximately [34-37]. According to this proposal, the change in electron energy, ΔE, associated with the interaction of atoms i and j is [7]:

$$\Delta E = \sum_p \left[Q_i Q_j / R_{ij} + (1/2)(\beta_{ij}^2)\sum_m\sum_n D_{mi}D_{n'j}/(E_m - E_{n'}) - (1/2)(\beta_{ij}^2)\sum_m\sum_{'n} D_{m'i}D_{nj}/(E_{m'} - E_n)\right] \qquad (5)$$

where Q_i is the net charge of atom i, F_{mi} is the Fukui index of atom i in MO m, β_{ij} is the resonance integral; and E_m ($E_{m'}$) is the energy of the m-th (m'-th) occupied (virtual) MO of molecule A, n and n' standing for molecule B. The value of β_{ij} is kept independent of the kind of AO because the A-B complex does not involve covalent bonds. The summation on p is over all pairs of interacting atoms. A recent analysis of the expression for Δε allowed us to incorporate several local atomic reactivity indices coming from Density Functional Theory [15, 38]. The final expression for Δε is:

$$\Delta\varepsilon \cong \sum_j \left[e_j Q_j + f_j S_j^E + s_j S_j^N \right] +$$
$$+\sum_j\sum_m \left[h_j(m)F_j(m) + x_j(m)S_j^E(m)\right] + \sum_j\sum_{m'}\left[r_j(m')F_j(m') + t_j(m')S_j^N(m')\right] +$$
$$+\sum_j \left[g_j\mu_j + k_j\eta_j + o_j\omega_j + z_j\varsigma_j + w_j Q_j^{\max}\right] \qquad (6)$$

where Q_i is the net charge of atom *i*, S_i^E and S_i^N are, respectively, the total atomic electrophilic and nucleophilic superdelocalizabilities of Fukui et al., $F_{i,m}$ is the Fukui index of atom i in occupied (empty) MO m (m'), $S_i^E(m)$ is the atomic electrophilic superdelocalizability of atom i in MO m, etc. [39]. The total atomic electrophilic superdelocalizability (ESD) of atom i is defined as the sum over occupied MOs of the $S_i^E(m)$'s and the total atomic nucleophilic superdelocalizability (NSD) of atom i is defined as the sum over empty MOs of the $S_i^N(m')$'s. S_i^E is related to the total electron-donating capacity of atom i and S_i^N to its total electron-accepting capacity. These indices are very helpful to compare the reactivity of a similar atomic position thought a series of molecules because they include the eigenvalue spectrum which is usually different in each molecular system [38]. The orbital components, $S_i^E(m)$ and $S_i^N(m')$, become significant when fine aspects of the drug-receptor interaction are needed for a more comprehensive elucidation of the interaction. The last bracket on the right side of Eq. 6 contains new local atomic indices obtained by an approximate rearrangement of part of the remaining terms of the series expansion employed in the model. μ_j, η_j, ω_j, ς_j and Q_j^{max} are, respectively, the local atomic electronic chemical potential of atom j, the local atomic hardness of atom j, the local atomic electrophilicity of atom j, the local atomic softness of atom j and the maximal amount of electronic charge that atom j may accept. The local atomic electronic chemical potential of atom i, μ_i, is defined as:

$$\mu_i = \frac{E_{oc}^* - E_{em}^*}{2} \qquad (7)$$

where E^* is the highest occupied MO with a non-zero Fukui index localized on atom i (called HOMO* hereafter) and E^* is the lowest empty MO with a non-zero Fukui index localized on atom i (called

ISSN 2291-6458 (Print), ISSN 2291-6466 (Online)
Year 2013 | Volume 1 | Issue 3 | Page 215-237

LUMO* hereafter). μ_i corresponds to the midpoint between the HOMO* and LUMO* energies. It is a measure of the tendency of an atom to gain or donate electrons; a large negative value indicates a good electron acceptor atom whereas a small negative value corresponds to a good electron donor atom.

The total local atomic hardness of atom i, η_i, is defined as:

$$\eta_i = E^*_{em} - E^*_{oc} \quad (8)$$

and corresponds to the distance between the energies of the local frontier molecular orbitals HOMO* and LUMO*. The local atomic hardness can be interpreted as the resistance of an atom to exchange electrons with the milieu.

The total local atomic softness of atom i, ς_i, is defined as the inverse of the local atomic hardness. The local electrophilic index of atom i, ω_i, is defined as:

$$\omega_i = \frac{\mu_i^2}{2\eta_i} \quad (9)$$

This index is related to the electrophilic power of an atom and includes the predisposition of the electrophile atom to receive extra electronic charge together with its resistance to exchange charge with the medium. The maximal amount of electronic charge that an electrophile may accept from another site, Q_i^{max}, is defined as:

$$Q_i^{max} = \frac{-\mu_i}{\eta_i} \quad (10)$$

The insertion of Eq. 6 into Eq. 4 leads to the master equation 11:

$$\log K_i = a + bM_{D_i} + c\log\left[\sigma_{D_i}/(ABC)^{1/2}\right] + \sum_j \left[e_j Q_j + f_j S_j^E + s_j S_j^N\right] +$$
$$+ \sum_j \sum_m \left[h_j(m)F_j(m) + x_j(m)S_j^E(m)\right] + \sum_j \sum_{m'} \left[r_j(m')F_j(m') + t_j(m')S_j^N(m')\right] +$$
$$+ \sum_j \left[g_j\mu_j + k_j\eta_j + o_j\omega_j + z_j\varsigma_j + w_j Q_j^{max}\right] \quad (11)$$

Then, for n molecules we have a system of n linear equations. *The most important attribute of these equations is that they contain terms associated only with the drug molecule*. Table 1 shows the local atomic indices and their proposed physical meaning. It was shown that the moment of inertia term of Eq. 11 it can be transformed into the approximate form [8,10]:

$$\log\left[(ABC)^{-1/2}\right] \simeq \sum_t \sum_t m_{i,t} R_{i,t}^2 = \sum_t O_t \quad (12)$$

where the summation over t is over the different substituents of the molecule, $m_{i,t}$ is the mass of the i-th atom belonging to the t-th substituent, $R_{i,t}$ being its distance to the atom to which the substituent is attached. This approximation allows us to transform a molecular property into a sum of substituent properties. We proposed that these terms represent the fraction of molecules attaining the proper orientation to interact with a given site. We have called them Orientation Parameters.

The second part of the problem is that there are many kinds of molecules that exert their biological actions through mechanisms involving two or more steps that may or may not include the passage through one or more membranes and/or pores, partition between two phases, etc. We know that the lipophilic properties of molecules can be modeled by their partition between organic and aqueous phases. We also accept that lipophilicity can be approximated by the water-octanol partition coefficient

ISSN 2291-6458 (Print), ISSN 2291-6466 (Online)
Year 2013 | Volume 1 | Issue 3 | Page 215-237

(log P). We face then the problem of providing a scientific basis for the possible modifications of Eq. 11 to describe the abovementioned processes. The only restriction we shall impose is that any modification of Eq. 11 must include only terms coming from the quantum-chemical realm.

Table 1: Local Atomic Reactivity Indices and their physical meaning.

Index	Name	Physical meaning
Q_i	Net atomic charge of atom i	Electrostatic interaction
S_i^E	Total atomic electrophilic superdelocalizability of atom i	Total atomic electron-donating capacity of atom i (MO-MO interaction)
S_i^N	Total atomic nucleophilic superdelocalizability of atom i	Total atomic electron-accepting capacity of atom i (MO-MO interaction)
$S_i^E(m)$	Orbital atomic electrophilic superdelocalizability of atom i and occupied MO m	Electron-donating capacity of atom i at occupied MO m (MO-MO interaction)
$S_i^N(m')$	Orbital atomic nucleophilic superdelocalizability of atom i and empty MO m’	Electron-accepting capacity of atom i at empty MO m’ (MO-MO interaction)
F_i	Fukui index of atom i	Total electron population of atom i (MO-MO interaction)
F_{mi}	Fukui index of atom i and occupied MO m.	Electron population of occupied MO m at atom i (MO-MO interaction)
$F_{m'i}$	Fukui index of atom i and empty MO m’	Electron population of empty MO m’ at atom i (MO-MO interaction)
μ_i	Local atomic electronic chemical potential of atom i	Propensity of atom i to gain or lose electrons
η_i	Local atomic hardness of atom i	Resistance of atom i to exchange electrons with a site
ς_i	Local atomic softness of atom i	The inverse of η_i
ω_i	Local atomic electrophilicity of atom i	Propensity of atom i to receive extra electronic charge together with its resistance to exchange charge with a site
$Q_i^{\max}$	Maximal amount of electronic charge atom i may receive	Maximal amount of electronic charge that atom i may receive from a donor site

In 1969 Cammarata and Rogers analyzed the partitioning of aromatic molecules between immiscible non polar-polar phases (water-saturated octanol/octanol-saturated water). For thirty aromatic molecules representing four chemical classes they found that the partition coefficients are correlated by a model equation that included the charge density and the induced polarization [40]. The same year both authors published a correlation between the partition coefficients of nineteen molecules and their charge density and total electrophilic superdelocalizability [41]. In 1971 the same group showed that the lipophilic parameter (π) values for benzoic acid substituents could be correlated with appropriate

ISSN 2291-6458 (Print), ISSN 2291-6466 (Online)
Year 2013 | Volume 1 | Issue 3 | Page 215-237

electronic indices calculated for the same substituents. They showed also that these same electronic indices were suitable for correlating the π values derived for phenoxyacetic acids [42]. Knowing that the most useful lipophilic indices are the logarithm of the partition coefficient or, in the case of congeneric series, the substituent constant π, we have generalized these results by stating the following hypothesis: *all biological processes occurring, from the moment of the entry of a drug molecule into the biological system* (*in vitro* or *in vivo*) *until the manifestation of any biological activity, are controlled by the local atomic reactivity indices appearing in Eq. 11*. Therefore, if this hypothesis is correct, *a preliminary representation of the final biological action can be obtained simply by replacing log* K_i *by log (BA)*, where *BA* is any biological *in vitro* or in *vivo activity*.

This is the working hypothesis we shall test in this study. Two previous studies give some support to this hypothesis. In the first one, good results were obtained for the relationship between accumulation capacity and molecular structure in a group of polychlorinated dibenzo-p-dioxins, polychlorinated dibenzofurans and polychlorinated biphenyls in some zucchini subspecies [13]. In a more recent study, we obtained good quality results concerning structure-biological activity relationships for two different sets of molecules presenting inhibitory activity against some effects of HIV-1 (inhibition of HIV-induced cytopathicity and cytostatic effects) and H1N1 virus (decrease of H1N1-induced cytopathic effects) [14]. These results are encouraging and seem to suggest that the approach used here is appropriate.

It is important to stress that our hypothesis covers multi-step (for example, in the n-th step molecules must cross a pore) and multimechanistic (for example, to cross the pore molecules must interact consecutively with j unknown sites) processes. Therefore it seems logical to state that a necessary condition to obtain good structure-activity relationships is that all the steps and all the mechanisms inside each step must be the same for all the group of molecules under study.

2.2. Selected Systems

We shall work within the *common skeleton hypothesis* stating that there is a certain group of atoms, common to all molecules analyzed (called the common skeleton), that accounts for almost all the binding to the receptor. The effect of the substituents consists in modifying the electronic structure of this skeleton and influencing the correct alignment of the drug through the orientational parameters. It is hypothesized that different parts of this entire common skeleton account for all interactions during a multi-step process leading to the manifestation of a given biological activity.

We analyzed two groups of molecules exerting different biological activities on distinct biological preparations. The first one is a group of "phenylaminopyridine" derivatives that inhibit HIV-1 replication [22]. Table 2 and Fig. 1 show these molecules, the common skeleton numbering and the corresponding experimental activities. The second system is a group of 1-azabenzanthrone derivatives displaying antiproliferative activity against normal human fibroblasts (MRC-5) and four human cancer cell lines (gastric adenocarcinoma AGS, lung cancer SK-MES-1, bladder carcinoma J82 and myelocytic leukemia HL-60 cells) [23]. Figure 2 and Table 3 display these molecules together with their corresponding experimental antiproliferative activities and the common skeleton numbering.

2.3 Calculations

The electronic structure of all molecules was calculated within Density Functional Theory (DFT) at the B3LYP/6-31g(d,p) (for phenylaminopyridine derivatives) and B3LYP/6-311g(d,p) (for 1-azabenzanthrone derivatives) levels of the theory. The Gaussian suite of programs was used [43]. The use of different basis sets was to test their value to produce reliable results. After full geometry optimization, verification that a local minimum was obtained and single point calculations, all the information necessary to obtain numerical values for all the local atomic reactivity indices of Eq. 11 was extracted

ISSN 2291-6458 (Print), ISSN 2291-6466 (Online)
Year 2013 | Volume 1 | Issue 3 | Page 215-237

from the Gaussian results with software written in our Laboratory. All electron populations smaller than or equal to 0.01 e were considered as zero [15]. Negative electron populations coming from Mulliken Population Analysis were corrected according to a newly proposed method [44]. Molecular orbitals and MEP were depicted using GaussView. Orientational parameters were calculated as usual. Since the solution of the system of linear equations is not possible because we do not have enough cases (i.e., molecules) we made use of Linear Multiple Regression Analysis (LMRA) techniques to find the best solution [45]. For each case, a matrix containing the dependent variable (the biological activity) and the local atomic reactivity indices of all atoms of the common skeleton as independent variables was built. The Statistica software was used for LMRA. It is important for the analysis to explain how the data matrix was built. Figure 3 shows atoms A, B and C and the localization of the frontier molecular orbitals on them.

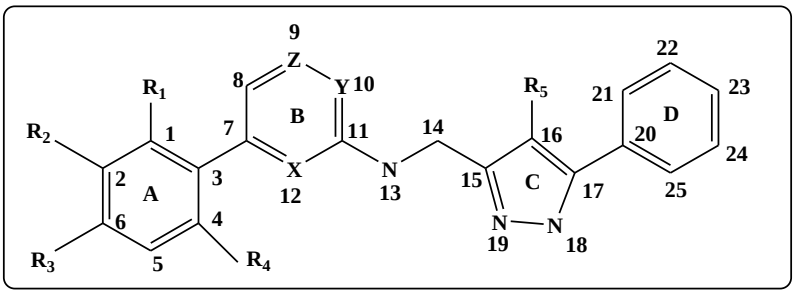

Figure 1. Phenylaminopyridine derivatives.

Table 2: Phenylaminopyridine derivatives and their biological activity.

Molecule	X	Y	Z	R_1	R_2	R_3	R_4	R_5	log EC_{50} (μM)
1	N	N	N	H	H	H	H	H	0.11
2	N	N	N	Me	H	H	H	H	-0.91
3	N	N	N	H	Me	H	H	H	0.36
4	N	N	N	Me	H	H	Me	H	-2.49
5	C	C	C	Me	H	H	H	H	0.34
6	C	C	N	Me	H	H	H	H	0.08
7	C	N	C	Me	H	H	H	H	-0.83
8	N	N	C	Me	H	H	H	H	-0.44
9	N	C	N	Me	H	H	H	H	-0.04
10	N	N	N	Me	H	CN	H	H	-2.77
11	C	C	N	Me	H	CN	H	H	-1.80
12	C	N	C	Me	H	CN	H	H	-3.10
13	N	N	C	Me	H	CN	H	H	-2.37
14	C	N	C	Me	H	CN	H	Cl	-2.17
15	C	N	C	Me	H	CN	H	H	-2.44
16	C	N	C	Me	H	CN	H	Cl	-3.70

ISSN 2291-6458 (Print), ISSN 2291-6466 (Online)
Year 2013 | Volume 1 | Issue 3 | Page 215-237

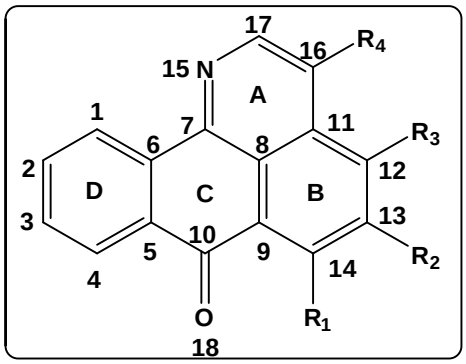

Figure 2. 1-azabenzanthrone derivatives.

Table 3: 1-azabenzanthrone derivatives and their antiproliferative activity.

Molecule	R1	R2	R3	R4	C_{16}-C_{17} bond	log(IC_{50}) MRC-5	log(IC_{50}) AG5	log(IC_{50}) SK-MES-1	log(IC_{50}) J82
1	H	H	H	H	Aromatic	1.62	1.52	----	1.97
2	OH	OMe	H	H	Aromatic	1.81	1.66	----	1.80
3	H	OMe	NH_2	H	Aromatic	1.57	----	----	----
4	NH_2	OMe	H	H	Aromatic	1.25	1.90	1.64	1.58
5	H	OMe	NO_2	H	Aromatic	1.01	0.65	1.23	1.40
6	NO_2	OMe	H	H	Aromatic	1.90	1.68	----	1.68
7	NO_2	OMe	NO_2	H	Aromatic	1.62	1.56	1.75	1.88
8	H	OMe	H	Br	Aromatic	1.46	0.52	0.96	0.38
9	H	OMe	Br	H	Aromatic	----	1.98	1.87	----
10	H	H	H	H	Single	1.46	0.18	1.46	-0.07
11	H	OMe	H	H	Single	1.93	0.83	1.26	0.48
12	OH	OMe	H	H	Single	1.63	0.59	1.87	0.76
13	OMe	H	H	H	Single	1.70	1.79	1.24	1.53
14	H	OMe	NO_2	H	Single	1.07	0.76	1.36	1.36
15	NO_2	OMe	H	H	Single	1.82	1.26	----	1.36
16	NO_2	OMe	NO_2	H	Single	1.56	-0.44	0.40	0.45

We may see that the molecular HOMO is localized on atoms A and B, but not on atom C. The LUMO is localized on atom A but not on atoms B and C. In atom A the "local" HOMO coincides with the molecular HOMO and the "local" LUMO corresponds to the molecular LUMO. In atom B the local HOMO is the same as the molecular HOMO, but the local LUMO corresponds to the molecular (LUMO+1) (i.e., the second highest empty MO). In atom C, the local HOMO corresponds to the third highest occupied MO (HOMO-2) and the local LUMO is the third highest empty molecular MO (LUMO+2). For these reasons we have denoted with an * the local MOs. Figure 4 shows, from left to right, the original matrix containing zero and non-zero Fukui indices, the matrix including only non-zero Fukui indices, and the local nomenclature. This applies also to all reactivity indices built from Fukui indices and/or MO energies.

ISSN 2291-6458 (Print), ISSN 2291-6466 (Online)
Year 2013 | Volume 1 | Issue 3 | Page 215-237

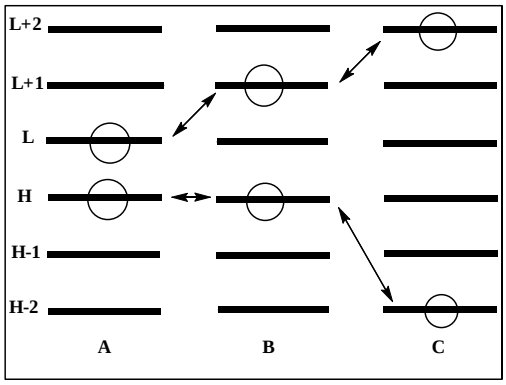

Figure 3. Localization of frontier MOs on atoms A, B and C. Circles depict the molecular MOs with non-zero electron populations. H corresponds to the HOMO, L to the LUMO and so on.

$$\left\{\begin{array}{ccc} A & B & C \\ F_A(L) & .... F_B(L) & .... F_C(L) \\ F_A(H) & .... F_B(H) & .... F_C(H) \end{array}\right\} \rightarrow \left\{\begin{array}{ccc} A & B & C \\ F_A(L) & .... F_B(L+1) & .... F_C(L+2) \\ F_A(H) & .... F_B(H) & ..... F_C(H-2) \end{array}\right\} \rightarrow \left\{\begin{array}{ccc} A & B & C \\ F_A(L)^* & .... F_B(L)^* & .... F_C(L)^* \\ F_A(H)^* & .... F_B(H)^* & .... F_C(H)^* \end{array}\right\}$$

Figure 4. From left to right: molecular frontier MOs, atomic frontier MOs and local nomenclature.

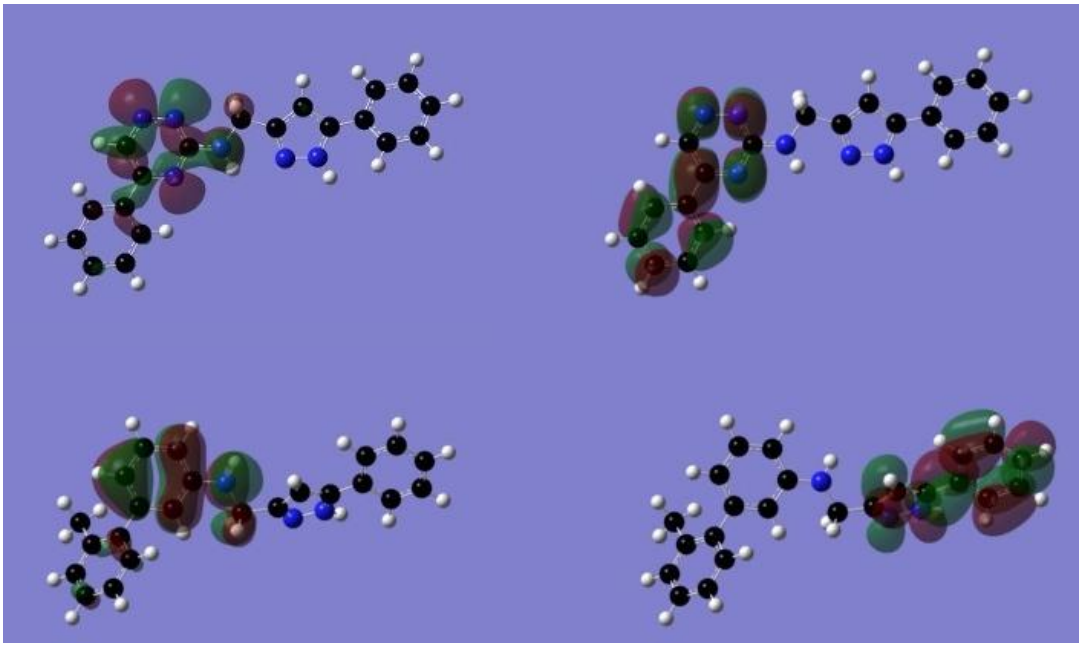

Figure 5: HOMO (left) and LUMO (right) localization in molecules 1 (upper) and 5 (lower). Isovalue = 0.02.

3. RESULTS AND DISCUSSION

3.1. Antiviral Activity of Phenylaminopyridine Derivatives

3.1.1. General Aspects of Electronic Structure

We have analyzed the localization of HOMO-1, HOMO, LUMO and LUMO+1 of all the molecules. No correlation, even approximate, was found between MO localization and biological activity. Figure 5 shows the localization of HOMO and LUMO of molecules 1 and 5. The HOMO and LUMO

ISSN 2291-6458 (Print), ISSN 2291-6466 (Online)
Year 2013 | Volume 1 | Issue 3 | Page 215-237

localization seems to be very different in these two molecules but, if we also consider the second highest occupied and empty MOs (which are not energetically far from the frontier MOs) a general similarity appears in all molecules. There are some points to comment on. The first is the high conformational flexibility of these systems. The molecular structure of the fully optimized molecules shows that we are in the presence of four aromatic regions connected in different ways. The region comprising rings A and B is separated from the ring C and D region by a CH_2 group. Therefore no π-electron transfer is expected between these regions. Steric hindrance (think of the biphenyl case) prevents the coplanarity of rings A and B and of rings C and D. If we remember that at body temperature these molecules can reach any conformation above 7 kcal/mol (provided that there are no high energy barriers) from the fully optimized structure, we have no solid base to propose what the conformation might be at each step of the process leading to the reported biological activity. When a π MO located on rings A and B is studied we may observe a small deformation of the electronic distribution in the region where the steric hindrance to rotation occurs. Also, when the number of nitrogen atoms increases in ring B we observe molecular orbitals with π character mixed with the nitrogen lone pairs. Figure 5 is helpful to understand the logic employed to build the variable matrix (see Fig. 1 for atom numbering). For example, in the case of molecules 1 and 5, the local HOMO (HOMO*) of atoms belonging to rings C and D does not coincide with the molecular HOMO. In molecule 5 the local HOMO of atoms belonging to ring D coincides with the molecular HOMO, but in molecule 1 it does not (in fact, in molecule 1 the local HOMO of ring D atoms corresponds to the molecular HOMO-1).

Figure 6 shows the molecular electrostatic potential of molecule 15 (with Cl and CN substituents). A positive MEP region encompasses part of ring A (due to the methyl substituent) and rings C and D. This is shown only as an example because, due to the arguments exposed above, we still have do not have a way of making a decision about the behavior of the MEP during the processes leading to biological activity.

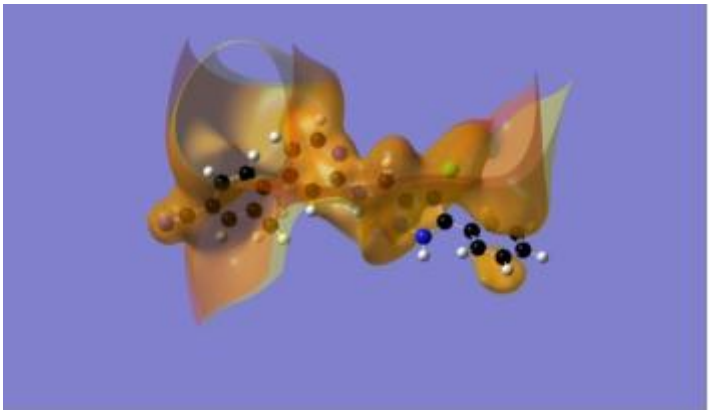

Figure 6. Molecular electrostatic potential of molecule 15. The orange isovalue surface corresponds to negative MEP values (-0.0004) and the yellow isovalue surface to positive MEP values (0.0004).

3.1.2. Relationship between Structure and Activity

Before presenting the results we must mention that the final equations correlate the *variation* of the biological activity with the *variation* of one or more local atomic reactivity indices. *Thus, any index making a constant contribution will not appear.*

The best equation obtained with the LMRA was:

$$\log(EC_{50}) = 11.62 - 11.17Q_6 + 40.83Q_5 - 12.11Q_{16}^{max} - 1.11F_4(LUMO + 2)^* \quad (13)$$

ISSN 2291-6458 (Print), ISSN 2291-6466 (Online)
Year 2013 | Volume 1 | Issue 3 | Page 215-237

with n=16, R=0.98, adj R^2=0.93, F(4,11)=54.85 (p<0.000001), outliers>2σ=0 and SD=0.35. Here Q_5 and Q_6 are, respectively, the net atomic charges of atoms 5 and 6, $F_4(LUMO+2)^*$ is the Fukui index of the (LUMO+2)* at atom 4 and Q_{16}^{max} is the maximal amount of charge that atom 16 may accept. The beta coefficients and t-test for significance of coefficients of Eq. 13 are shown in Table 4. Concerning independent variables, Table 5 shows that there are no significant internal correlations with the exception of $r^2\{Q_6, Q_{16}^{max}\}$=0.4. Figure 7 shows the plot of observed values *vs.* calculated ones. The associated statistical parameters of Eq. 13 show that this equation is statistically significant and that the variation of a group of local atomic reactivity indices belonging to the common skeleton explains about 93% of the variation of the biological activity.

Table 4: Beta coefficients and *t*-test for significance of coefficients in Eq. 13.

Variable	Beta	t(11)	p-level
Q_6	-0.80	-8.84	<0.000003
Q_5	0.35	4.51	<0.0009
Q_{16}^{max}	-0.35	-4.04	<0.002
$F_4(LUMO+2)^*$	-0.17	-2.24	<0.05

Table 5. Squared correlation coefficients for the variables appearing in Eq. 13.

	Q_5	$F_4(LUMO+2)^*$	Q_6
$F_4(LUMO+2)^*$	0.07	1.00	
Q_6	0.07	0.1	1.00
Q_{16}^{max}	0.008	0.1	0.4

Note that the standard error of estimate is 0.35, a high value that is not normally obtained in theoretical studies of 1:1 *in vitro* drug-receptor interactions. The correlation between Q_6 and Q_{16}^{max} is relatively high but note that atoms 6 and 16 belong to different and not electronically connected aromatic regions (rings A and C respectively). Beta values indicate that the importance of the variables of Eq. 13 is $Q_6 >> Q_5 \sim Q_{16}^{max} >> F_4(LUMO+2)^*$ (Table 4). These results are in agreement with the results of the *t*-test (Table 4). Therefore, our results indicate that the variation of log(EC_{50}) is associated with the variation of four local atomic reactivity indices located at atoms 4, 5, 6 and 16 of the common skeleton (see Fig. 1). Note that these good results were obtained after a number of approximations made to build the formal model relating structure with activity, without any knowledge of the exact conformation adopted by the molecules during the processes leading to the manifestation of biological activity and despite the complexity of the test to measure the inhibition of HIV-1 replication (i.e., CEMx174-LTR-GFP cells were seeded with a microplate dispenser at a density of 4,000 cells/well into 384-well glass plates pre-dispensed with 10 μL of compound diluted in DMSO and incubated for 1 h at 37 °C, 5% CO_2. Then cells

ISSN 2291-6458 (Print), ISSN 2291-6466 (Online)
Year 2013 | Volume 1 | Issue 3 | Page 215-237

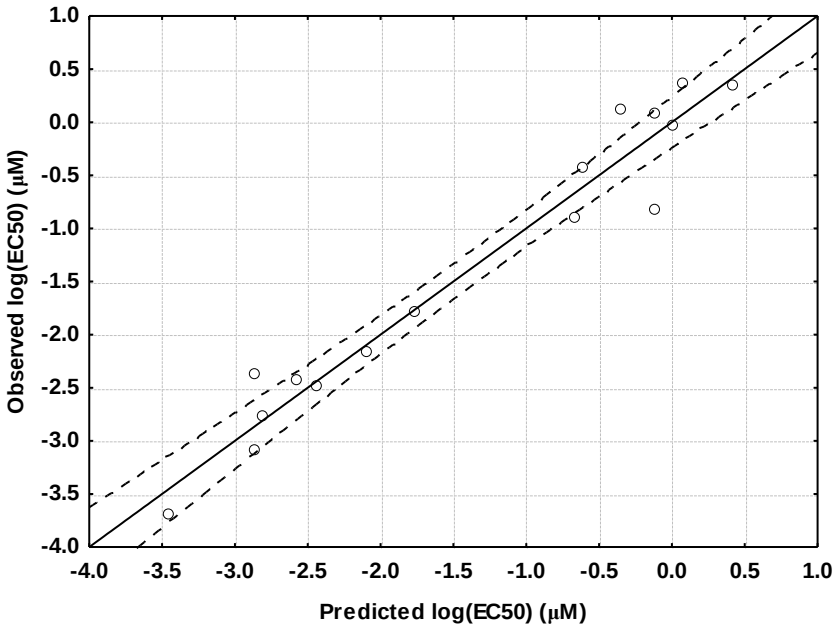

Figure 7: Observed versus calculated values (Eq. 13) of log (EC_{50}). Dashed lines denote the 95% confidence interval.

were infected with HIV-1LAI at a multiplicity of infection of 3 and incubated for 5 days at 37 °C, 5% CO_2. Fluorescence intensities were determined using a multilabel plate reader. Taken from Suppl. Mat. of Ref. [22]). Eq. 13 shows that the whole process is charge- and orbital-controlled. A variable-by-variable analysis indicates that good replication inhibitory activity is associated with a positive net charge on atom 6, a negative net charge on atom 5, a high capability for charge acceptance by atom 16 and a high value of the Fukui index of atom 4 at the third empty MO* (see Fig 1 for common skeleton numbering). Three of the four reactivity indices are located on ring A and the remaining one belongs to ring C. Remembering that the data matrix for the LMRA included only non-zero values for the Fukui indices (and superdelocalizabilities) we may infer that the three empty MOs located on atom 4 (all of π character) are participating in a charge transfer interaction with a rich electron-donor center. Starting from the definition of Q_i^{max} (i.e., $Q_i^{max} = -\mu_i / \eta_i$), a high numerical value for this index can be obtained by lowering the $HOMO_i$*-$LUMO_i$* gap (η_i) and the eigenvalue of $HOMO_i$* (i.e., making larger the numerical for $|\mu_i|$). Translated into MO language, this means that atom 16 should have a reactive LUMO* with an energy close to zero and a HOMO* with an energy far from zero. Knowing that the HOMO* and LUMO* of atom 16 are both of π nature we may suppose that this atom (and probably the ring including it) is participating as an electron acceptor with an electron-donor site (for example through a halogen bonding with an oxygen atom). The net charges of atoms 5 and 6 suggest that an electrostatic interaction with a complementary site takes place. Note also that, within an alternative model for a substituted benzene molecule, the optimal numerical values for the variables of atoms 4, 5 and 6 are compatible. The two-dimensional (2D) interaction pharmacophore built with the above data is shown in Fig. 8.

ISSN 2291-6458 (Print), ISSN 2291-6466 (Online)
Year 2013 | Volume 1 | Issue 3 | Page 215-237

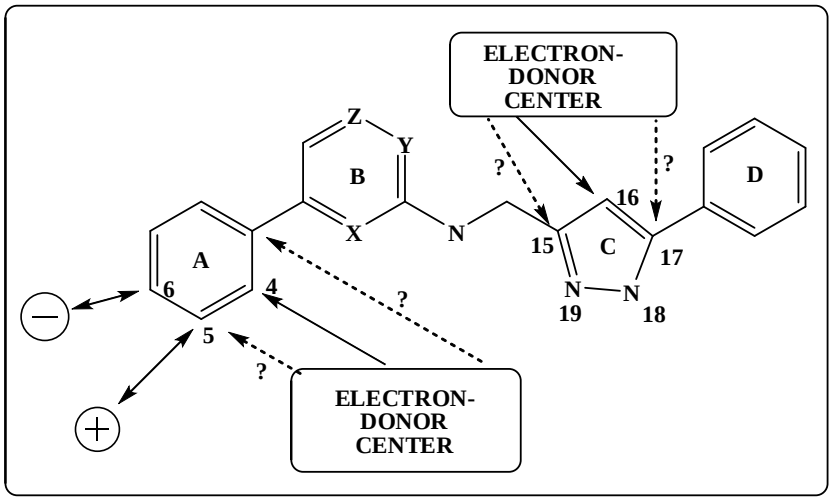

Fig. 8. 2D interaction pharmacophore for the inhibition of HIV-1 replication (the ? symbol indicates a possible π-π interaction involving more than one atom of rings A and C.

3.2. Inhibition of Cell Growth by 1-Azabenzanthrone Derivatives

3.2.1. General Comments

These molecules form an interconnected four-ring system. All highest occupied and lowest empty molecular orbitals are localized on it. The actual localization is controlled by the substituents and, in several cases by the hydrogenation of positions 16 and 17 of the common skeleton (see Fig. 2). Figures 9 and 10 show, respectively, the HOMO and LUMO of molecules 1 and 10.

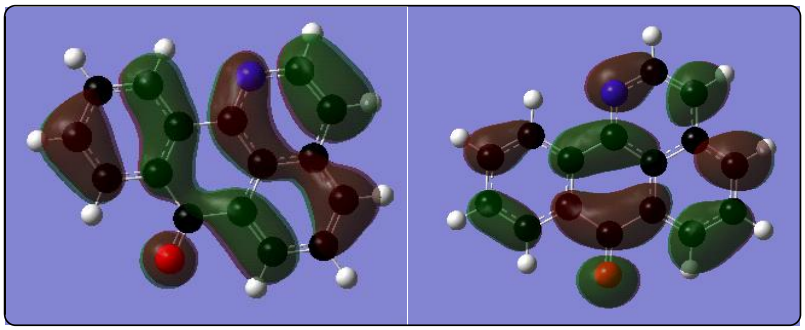

Figure 9. HOMO (left) and LUMO (right) of molecule 1 (isovalue = 0.02).

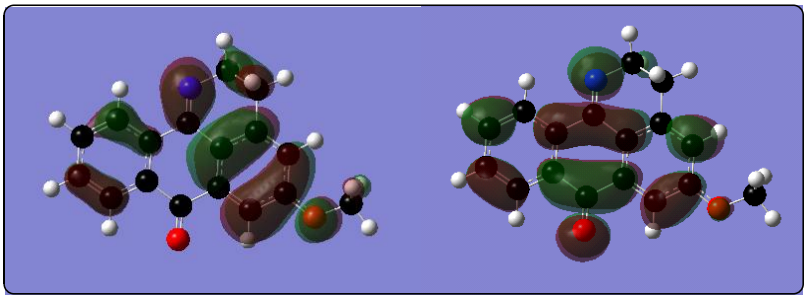

Figure 10. HOMO (left) and LUMO (right) of molecule 10 (isovalue = 0.02).

ISSN 2291-6458 (Print), ISSN 2291-6466 (Online)
Year 2013 | Volume 1 | Issue 3 | Page 215-237

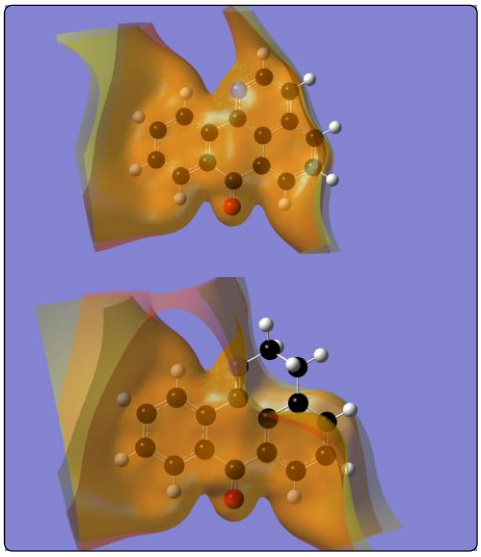

Figure 11. MEP of molecules 1 (upper) and 10 (lower). The orange isovalue surface corresponds to negative MEP values (-0.0004) and the yellow isovalue surface to positive MEP values (0.0004)

Note that the HOMOs (of π character) of these two molecules are very different. For example, in ring C part of the HOMO is localized on atom 10 of the common skeleton (see Fig. EE) in molecule 1 but it is not in molecule 10. The LUMOs are similar in both molecules, with the exception of small differences on atoms 1 and 17.

Regarding the molecular electrostatic potential, Figure 11 shows the MEP for molecules 1 and 10. The MEP maps are very similar with the exception that a large area of positive potential appears at the upper right hand side of molecule 10 as a result of the hydrogenation of two carbon atoms of ring A.

Before analyzing the structure-activity results we must mention that no linear relationship exists between any pair of sets of experimental values (see below).

3.2.2. Gastric Adenocarcinoma (AGS) Cells

The best statistical equation obtained was:

$$\log(IC_{50}) = 0.93 - 0.52S_{16}^{N}(LUMO)^{*} - 0.005\phi_{R4} - 0.44S_{2}^{E}(HOMO-1)^{*} - 5.65F_{4}(HOMO)^{*} \quad (14)$$

with n=15, R=0.97, adj. R^2=0.92, F(4,10)=39.80 (p<0.000001), outliers>2σ=0 and SD=0.21. Here, ϕ_{R4} is the orientational effect of the R_4 substituent, $S_{16}^{N}(LUMO)^{*}$ is the nucleophilic superdelocalizability of atom 16 at LUMO* level, $S_{2}^{E}(HOMO-1)^{*}$ is the electrophilic superdelocalizability of atom 2 at (HOMO-1)* level and $F_{4}(HOMO)^{*}$ is the Fukui index of atom 4 at the HOMO* level. The beta coefficients and *t*-test for the significance of coefficients of Eq. 14 are shown in Table 6. Concerning independent variables, Table 7 shows that there are no significant internal correlations. Figure 12 shows the plot of observed values *vs.* calculated ones. The associated statistical parameters of Eq. 14 show that this equation is statistically significant and that the variation of a group of local atomic reactivity indices belonging to the common skeleton explains about 92% of the variation of the antiproliferative activity.

The standard error of estimate is 0.21, a value that is normally obtained in theoretical studies of

ISSN 2291-6458 (Print), ISSN 2291-6466 (Online)
Year 2013 | Volume 1 | Issue 3 | Page 215-237

Table 6: Beta coefficients and *t*-test for significance of coefficients in Eq. 14.

	Beta	t(10)	p-level
$S_{16}^{N}(LUMO)*$	-0.71	-7.58	<0.00002
ϕ_{R4}	-0.51	-6.33	<0.00009
$S_{2}^{E}(HOMO-1)*$	-0.42	-5.27	<0.0004
$F_{4}(HOMO)*$	-0.32	-3.52	<0.006

Table 7: Squared correlation coefficients for the variables appearing in Eq. (XX).

	$S_{2}^{E}(HOMO-1)*$	$F_{4}(HOMO)*$	$S_{16}^{N}(LUMO)*$
$F_{4}(HOMO)*$	0.0004	1.00	
$S_{16}^{N}(LUMO)*$	0.004	0.3	1.00
ϕ_{R4}	0.04	0.01	0.06

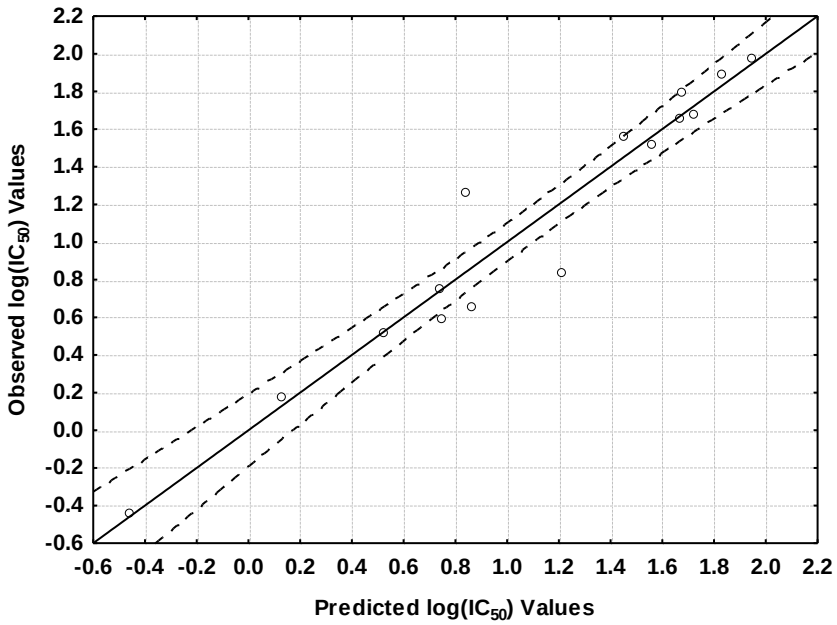

Figure 12: Observed versus calculated values (Eq. 14) of log(IC_{50}) for AGS cells. Dashed lines denote the 95% confidence interval.

1:1 *in vitro* drug-receptor interaction. A fairly high correlation exists between $S_{16}^{N}(LUMO)*$ and $F_{4}(HOMO)*$ (Table 7). The beta values show that the order of importance of the variables of Eq. 14 is $S_{16}^{N}(LUMO)*>\phi_{R4}>\ S_{2}^{E}(HOMO-1)*\ >F_{4}(HOMO)*$ (Table 6), these results being in agreement with the results of the *t*-test (Table 6). Therefore, our results indicate that the variation of log(IC_{50}) is associated with the variation of three local atomic reactivity indices located at atoms 2, 4 and 16 of the

ISSN 2291-6458 (Print), ISSN 2291-6466 (Online)
Year 2013 | Volume 1 | Issue 3 | Page 215-237

common skeleton and with the variation of the orientational parameter of the R_4 substituent (see Fig. 2). The whole process is orbital- and orientational-parameter-controlled [36]. A variable-by-variable analysis indicates that good inhibitory activity is associated with high values of ϕ_{R4} and $F_4(HOMO)^*$, a low value of $S_2^E(HOMO-1)^*$ and a positive numerical value for $S_{16}^N(LUMO)^*$. Three of the four reactivity indices are located on ring D and the remaining one on ring A. It is interesting to note that the three indices on ring D are electronic, while the orientational parameter of the substituent (that is only mass- and distance-dependent) pertains to ring A. Therefore, and for this specific biological process, it seems that the MEP structure around ring A may undergo perceptible changes that do not disturb the entire process (see Fig. 11). Regarding the high value for ϕ_{R4} we must note that the only R_4 substituents employed for the LMRA are hydrogen and bromine. The problem for the experimental medicinal chemist is then to find an R_4 substituent with a large orientational parameter that affects the electronic structure of the aromatic system approximately the same as H and Br. A high value for $F_4(HOMO)^*$ and the π nature of this MO suggest that atom 4 acts as an electron donor site.

In *ab initio* and DFT calculations one or more empty MOs sometimes have a negative orbital energy. When this happens, the numerical values for the total nucleophilic superdelocalizability are not reliable because the negative terms will annihilate algebraically with some positive terms. When using the frontier nucleophilic superdelocalizabilities we encountered the problem of having a set of negative and positive numerical values clouding the interpretation of the statistical equations. With these considerations, and because almost (but not all) all the $S_{16}^N(LUMO)^*$ values are positive; we made the suggestion that $S_{16}^N(LUMO)^*$ values are positive. In any case, the (LUMO)* of atom 16 should act as an electron acceptor site. In the future we shall test the idea of shifting the zero MO energy to the Fermi level (i.e., the midpoint between the HOMO and LUMO energies) only with the purpose of calculating the nucleophilic superdelocalizabilities. A low numerical value for $S_2^E(HOMO-1)^*$ is required. Knowing that for all molecules studied here the HOMO* and (HOMO-1)* of atom 2 are of π nature, a low value for $S_2^E(HOMO-1)^*$ could be interpreted proposing that this atom is engaged as an electron donor in a π-π interaction with a complementary site but that its second inner π MO (the (HOMO-1)*) is hampering it. Therefore the general requirement for the (HOMO-1)* of atom 2 is that the associated eigenvalue be more negative or that its Fukui index be numerically low. If we note that atoms 2 and 4 (see Fig. 2) are engaged as electron donors we may hypothesize that, within an alternant model of conjugated π systems, the whole ring D could be participating in a π-π interaction with a complementary site. Fig. 13 shows the corresponding 2D antiproliferative pharmacophore.

3.2.3. Bladder carcinoma (J82) Cells

The best statistical equation obtained was:

$$\log(IC_{50}) = -0.56 + 1.03F_2(HOMO)^* - 5.32F_5(HOMO)^* - 13.56\mu_{16} - 0.004\phi_{R4} \quad (15)$$

with n=14, R=0.99, adj. R^2=0.96, F(4,9)=85.84 ($p<0.000001$), outliers>2σ=0 and SD=0.13. Here, ϕ_{R4} is the orientational effect of the R_4 substituent, μ_{16} is the local electronic chemical potential of atom 16, $F_2(HOMO)^*$ and $F_5(HOMO)^*$ are, respectively, the Fukui indices of atoms 2 and 5 at their

ISSN 2291-6458 (Print), ISSN 2291-6466 (Online)
Year 2013 | Volume 1 | Issue 3 | Page 215-237

(HOMO)* level. The beta coefficients and *t*-test for the significance of coefficients of Eq. 15 are shown in Table 8. Concerning independent variables, Table 9 shows that there are no significant internal correlations. Figure 14 shows the plot of observed values *vs.* calculated ones. The associated statistical parameters of Eq. 15 show that this equation is statistically significant and that the variation of a group of local atomic reactivity indices belonging to the common skeleton explains about 96% of the variation of the antiproliferative activity.

The beta values show that the order of importance of the variables of Eq. 14 is $\mu_{16} > \phi_{R4} > F_5(HOMO)^* \sim F_2(HOMO)^*$ (Table 8), these results being in agreement with the results of the *t*-test. No significant correlation exists between independent variables (Table 9). Therefore, our results indicate that the variation of log(IC_{50}) is associated with the variation of three local atomic reactivity indices

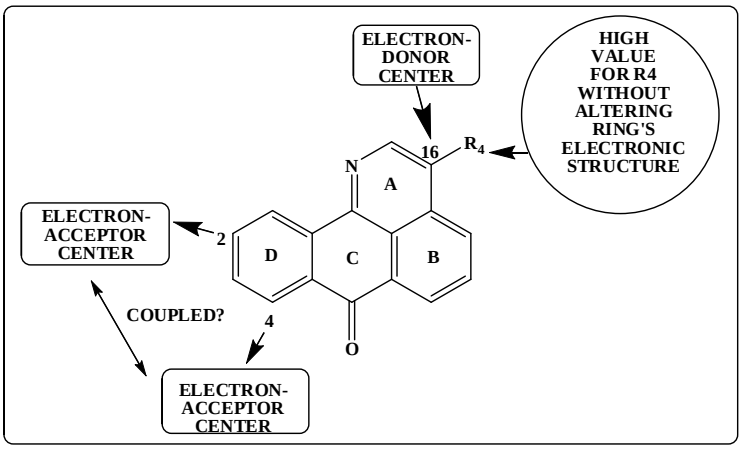

Figure 13. 2D pharmacophore for the antiproliferative activity of 1-azabenzanthrone derivatives in gastric adenocarcinoma cells.

Table 8: Beta coefficients and *t*-test for significance of coefficients in Eq. 15.

	Beta	t(9)	p-level
$F_2(HOMO)^*$	0.25	4.56	<0.002
$F_5(HOMO)^*$	-0.26	-4.61	<0.001
μ_{16}	-0.89	-15.07	<0.0000001
ϕ_{R4}	-0.46	-8.50	<0.00001

Table 9: Squared correlation coefficients for the variables appearing in Eq. 15.

	$F_2(HOMO)^*$	$F_5(HOMO)^*$	μ_{16}
$F_5(HOMO)^*$	0.01	1.00	
μ_{16}	0.03	0.1	1.00
ϕ_{R4}	0.008	0.0004	0.02

ISSN 2291-6458 (Print), ISSN 2291-6466 (Online)
Year 2013 | Volume 1 | Issue 3 | Page 215-237

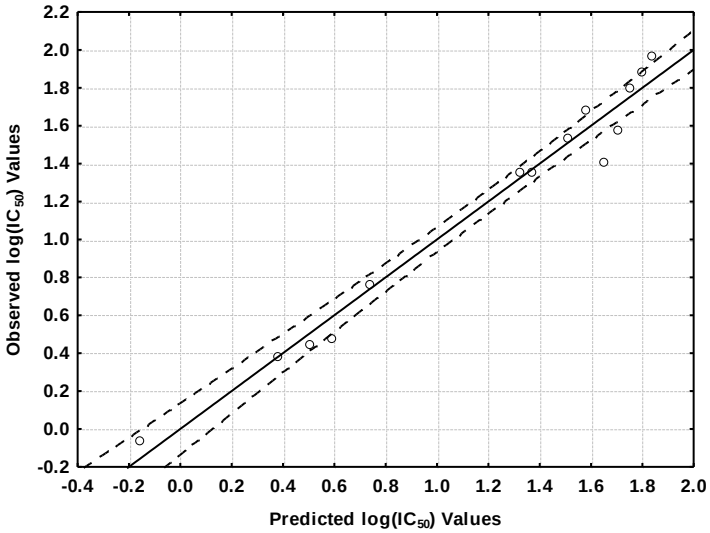

Figure 14: Observed versus calculated values (Eq. 15) of log(IC_{50}) for J82 cells. Dashed lines denote the 95% confidence interval.

located at atoms 2, 5 and 16 of the common skeleton and with the variation of the orientational parameter of the R_4 substituent (see Fig. 2). The whole process is energy-, orbital- and orientational-parameter-controlled [36]. Good inhibitory activity is associated with high values of ϕ_{R4} as in Eq. 14. In Eq. 15 a small value for μ_{16} indicates that atom 16 should act as an electron donor. In Eq. 14 atoms 16 acts as an electron-acceptor. A high value is required for $F_5(HOMO)^*$ indicating that this atom acts as an electron donor center (given that the (HOMO)* of atom 5 is of π nature it is likely that ring D participates in a π-π interaction with another π system such as a phenyl, carbonyl or carboxylate counterpart). Interestingly, atom 2 should have a low electron population at the (HOMO)* level (i.e., a low $F_2(HOMO)^*$ value). However, considering the low beta values for $F_2(HOMO)^*$ and $F_5(HOMO)^*$, we shall abstain from doing a deeper analysis of these indices. Figure 15 shows the corresponding 2D pharmacophore.

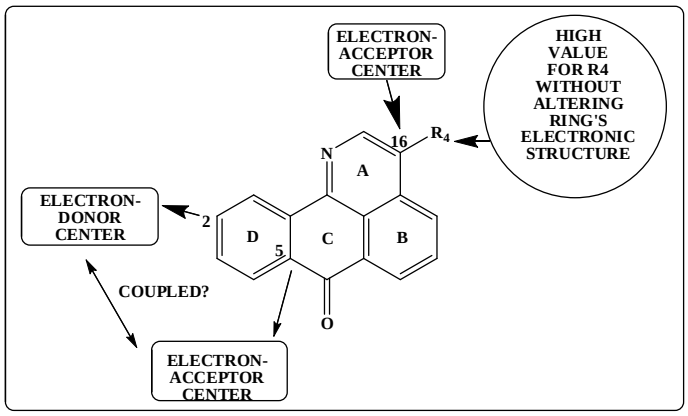

Figure 15. 2D pharmacophore for antiproliferative activity of 1-azabenzanthrone derivatives in bladder carcinoma cells.

ISSN 2291-6458 (Print), ISSN 2291-6466 (Online)
Year 2013 | Volume 1 | Issue 3 | Page 215-237

Table 10: Beta coefficients and *t*-test for significance of coefficients in Eq. 16.

	Beta	t(10)	p-level
$F_{10}(LUMO)*$	0.61	5.28	<0.0004
$S_{15}^{E}(HOMO)*$	0.57	5.42	<0.0003
$F_{15}(LUMO+2)*$	-0.38	-3.08	<0.01
ϕ_{R1}	0.29	2.70	<0.02

Table 11: Squared correlation coefficients for the variables appearing in Eq. 16.

	$F_{10}(LUMO)*$	$F_{15}(LUMO+2)*$	$S_{15}^{E}(HOMO)*$
$F_{15}(LUMO+2)*$	0.2	1.00	
$S_{15}^{E}(HOMO)*$	0.1	0.07	1.00
ϕ_{R1}	0.006	0.1	0.006

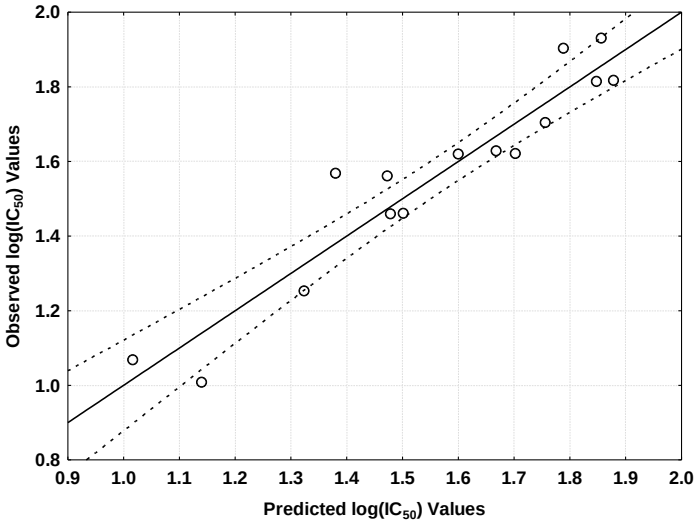

Figure 16: Observed versus calculated values (Eq. 16) of log(IC_{50}) for MRC-5 cells. Dashed lines denote the 95% confidence interval.

3.2.4. Normal human Fibroblasts (MRC-5 cells)

The best statistical equation obtained was:

$$\log(IC_{50}) = 0.95 + 4.08F_{10}(LUMO)* + 0.30S_{15}^{E}(HOMO)* - 1.77F_{15}(LUMO+2)* + 0.0003\phi_{R1} \quad (16)$$

with n=15, R=0.95, adj. R^2=0.86, F(4,10)=23.13 (p<0.00001), outliers>2σ=0 and SD=0.10. Here, ϕ_{R1} is the orientational parameter of the R_1 substituent, $S_{15}^{E}(HOMO)*$ is the electrophilic superdelocalizability of atom 15 at the HOMO* level, $F_{10}(LUMO)*$ and $F_{15}(LUMO+2)*$ are the Fukui indices of atoms

ISSN 2291-6458 (Print), ISSN 2291-6466 (Online)
Year 2013 | Volume 1 | Issue 3 | Page 215-237

10 and 15 at the (LUMO)* and (LUMO+2) molecular orbitals. The beta coefficients and *t*-test for significance of coefficients of Eq. 16 are shown in Table 10. Concerning independent variables, Table 11 shows that there are no significant internal correlations. Figure 16 shows the plot of observed values *vs.* calculated ones. The associated statistical parameters of Eq. 16 show that this equation is statistically significant and that the variation of a group of local atomic reactivity indices belonging to the common skeleton explains about 86% of the variation of the antiproliferative activity.

The beta values show that the order of importance of the variables of Eq. 14 is $F_{10}(LUMO)^* \sim S_{15}^{E}(HOMO)^* > F_{15}(LUMO+2)^* \sim \phi_{R1}$ (Table 10), these results being in agreement with the results of the *t*-test. No significant correlation exists between independent variables (Table 11). Therefore, our results indicate that the variation of log(IC_{50}) is associated with the variation of three local atomic reactivity indices located at atoms 1, 10 and 15 of the common skeleton and with the variation of the orientational parameter of the R_1 substituent (see Fig. 2). The whole process is orbital- and orientational-parameter-controlled [36]. A high value required for $S_{15}^{E}(HOMO)^*$ points to the participation of atom 15 as an electron donor center. In this particular case we cannot assert if atom 15 is participating in a hydrogen bond (with a hydroxyl group for example) or in a π-π interaction. The low value for $F_{10}(LUMO)^*$ suggests that atom 10 could be facing a region possessing empty MOs. This repulsive interaction seems to diminish the antiproliferative activity. For the index $F_{15}(LUMO+2)^*$ a high value is optimal. Knowing that the (LUMO)*, (LUMO+1)* and (LUMO+2)* are of π nature it is clear that atom 15 is interacting with an electron-rich center acting as an electron acceptor. At a first sight it would seem that the two indices for atom 15 (a nitrogen atom, see Fig. 2) appearing in Eq. 16 are contradictory: the N atom seems to act as an electron donor and an electron acceptor. Nevertheless this is only a clear example of the simple fact that, this being an unknown multi-step process, the N atom surely interacts in both ways but at different stages. Note that the beta value for $S_{15}^{E}(HOMO)^*$ is higher than the beta value for $F_{15}(LUMO+2)^*$. The small value for ϕ_{R1} has a low beta but we may speculate that the synthesis of new molecules with a methyl or ethyl group at R_1 could help to elucidate the correct size of this substituent. Figure 17 shows the 2D pharmacophore.

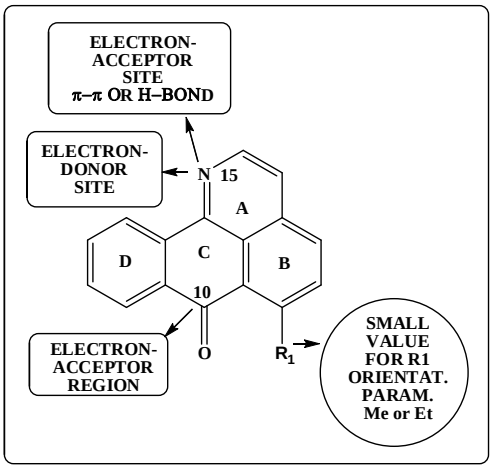

Figure 17. 2D pharmacophore for antiproliferative activity of 1-azabenzanthrone derivatives in normal human fibroblasts (MRC-5 cells).

ISSN 2291-6458 (Print), ISSN 2291-6466 (Online)
Year 2013 | Volume 1 | Issue 3 | Page 215-237

3.2.5. Lung Cancer (SK-MES-11) Cells

The best statistical equation obtained was:

$$\log(IC_{50}) = 2.03 - 5.77F_{10}(HOMO-2)^* + 1.27S_{11}^E(HOMO-2)^* + 0.94S_8^E(HOMO-2)^* + 0.95F_8(HOMO)^* \quad (17)$$

with n=11, R=0.98, adj. R^2=0.95, F(4,6)=47.91 (p<0.0001), outliers>2σ=0 and SD=0.10. Here, $F_{10}(HOMO-2)^*$ is the Fukui index of atom 10 at MO (HOMO-2)*, $S_{11}^E(HOMO-2)^*$ is the electrophilic superdelocalizability of atom 11 at the (HOMO-2)* MO, $S_8^E(HOMO-2)^*$ is the electrophilic superdelocalizability of atom 8 at MO (HOMO-2)* and $F_8(HOMO)^*$ is the Fukui index of atom 8 at the (HOMO)* MO. The beta coefficients and *t*-test for the significance of coefficients of Eq. 17 are shown in Table 12. Concerning independent variables, Table 13 shows that there are no significant internal correlations with the exception of the couple $S_8^E(HOMO-2)^*$ - $F_{10}(HOMO-2)^*$ (r^2=0.3). Figure 18 shows the plot of observed values *vs.* calculated ones. The associated statistical parameters of Eq. 17 show that this equation is statistically significant and that the variation of a group of local atomic reactivity indices belonging to the common skeleton explains about 95% of the variation of the antiproliferative activity.

Table 12: Beta coefficients and *t*-test for significance of coefficients in Eq. 17.

Variable	Beta	t(6)	p-level
$F_{10}(HOMO-2)^*$	-0.28	-3.20	<0.02
$S_{11}^E(HOMO-2)^*$	0.69	9.30	<0.00009
$S_8^E(HOMO-2)^*$	0.51	5.72	<0.001
$F_8(HOMO)^*$	0.28	3.91	<0.008

Table 13: Squared correlation coefficients for the variables appearing in Eq. 17.

	$F_8(HOMO)^*$	$S_8^E(HOMO-2)^*$	$F_{10}(HOMO-2)^*$
$S_8^E(HOMO-2)^*$	0.01	1.00	
$F_{10}(HOMO-2)^*$	0.003	0.3	1.00
$S_{11}^E(HOMO-2)^*$	0.001	0.04	0.003

The beta values show that the importance of the variables of Eq. 17 varies in the order $S_{11}^E(HOMO-2)^*$ > $S_8^E(HOMO-2)^*$ > $F_{10}(HOMO-2)^*$ ~ $F_8(HOMO)^*$ (Table 12), these results being in agreement with the results of the *t*-test. Therefore, our results indicate that the variation of log(IC_{50}) is associated with the variation of four local atomic reactivity indices located at atoms 8, 10 and 11 of the common skeleton (see Fig. 2). The whole process is orbital-controlled [36]. A high value of $S_{11}^E(HOMO-2)^*$ is required for optimal antiproliferative activity. The (HOMO)* for atom 11 is of π nature in all the molecules. A minority of the (HOMO-1)* values at atom 11 are of a π character while the

ISSN 2291-6458 (Print), ISSN 2291-6466 (Online)
Year 2013 | Volume 1 | Issue 3 | Page 215-237

rest are of σ nature. When a (HOMO-1)* is of σ character the (HOMO-2)* is of π character and vice versa. Noting that almost all the (HOMO-2)* are π we suggest then that atom 11 is participating with its first two π MOs in a charge transfer as an electron donor. A high value of $S_8^E(HOMO-2)*$ is required for optimal activity. The distribution of the three highest occupied local MOs at this atom is similar to the case of atom 11. Therefore atom 8 could also participate with its first two π MOs in a charge transfer as an electron donor. A low numerical value for $F_8(HOMO)*$ suggests that, in another step leading to the manifestation of biological activity, these molecules should have a low populated (HOMO)*, probably because they reach a region rich in electron-donor sites. Then, if both conditions are obligatory, the experimentalist should find a balance between these two requirements. A high value for $F_{10}(HOMO-2)*$, together with a similar distribution of the three highest local occupied MOs at atoms 8 and 11, suggest that atom 10 is also acting as an electron donor. Figure 19 displays the corresponding 2D pharmacophore.

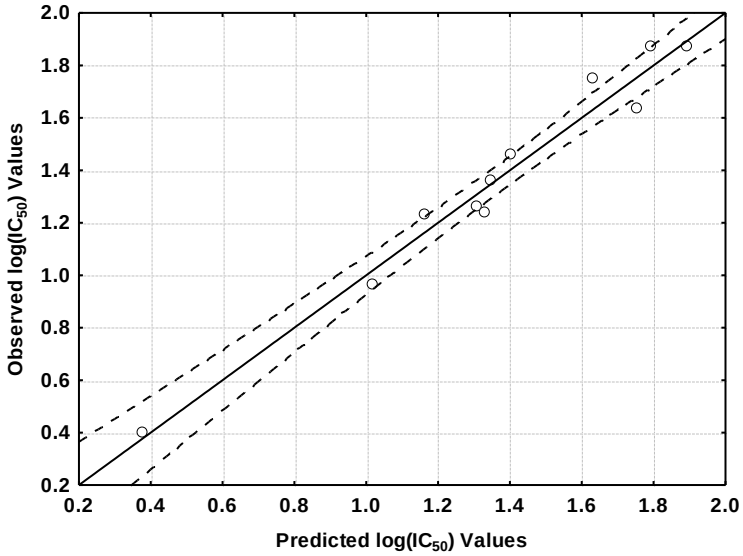

Figure 18: Observed *vs.* calculated values (Eq. 17) of log(IC_{50}) for SK-MES-11 cells. Dashed lines denote the 95% confidence interval.

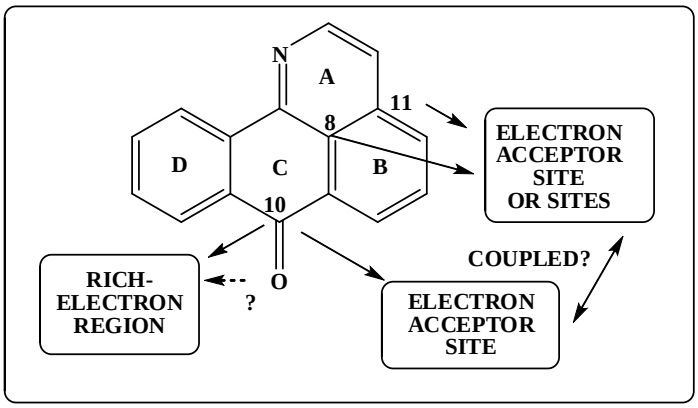

Figure 19. 2D pharmacophore for antiproliferative activity of 1-azabenzanthrone derivatives in lung cancer (SK-MES-11) cells.

ISSN 2291-6458 (Print), ISSN 2291-6466 (Online)
Year 2013 | Volume 1 | Issue 3 | Page 215-237

Given the structure of equations 14-17 we suggest that 1-azabenzanthrone derivatives exert their antiproliferative action on these four cell lines through different mechanisms. If this assertion is true then the medicinal chemist should target one cell line at a time when considering one particular mechanism, and look for more specific compounds. It is interesting to note that ring A is not necessary for antiproliferative action because some anthracene-9,10-diones also show the same kind of biological activity. For each cell line all molecules seem to undergo the same steps and interactions leading to growth inhibition. Finally, it is possible to observe in Figs. 7, 12, 14 and 16 that several cases are outside the 95% confidence interval. This can be interpreted by suggesting that, despite of the fact that the common skeleton gives an account of almost all the biological activity, in these cases one or more interactions could occur directly via the substituents. Recent QSAR results obtained by us on cannabinoids (in press) and hepatitis C virus replicon inhibitors (unpublished) support this statement.

4. CONCLUSIONS

The general hypothesis that any *in vitro* or *in vivo* biological activity can be explained only in terms of local atomic reactivity indices has been proposed and tested for five cases. In all cases good structure-activity relationships have been obtained and some requirements for potent biological activity have been suggested. For the cases tested here the common skeleton hypothesis works well. As this hypothesis has a logical conceptual basis but does not yet have a formal general mathematical background, it cannot be generalized and must be tested case by case. This methodology gives an account of the whole process and, in the case of multi-step processes, is unable to relate the different reactivity indices appearing in the SAR equations to any particular step. Nevertheless it opens a new field for non-empirical structure-activity research.

REFERENCES AND NOTES

[1] Martin, Y. C. Quantitative drug design : a critical introduction; M. Dekker: New York, 1978.
[2] Gómez Jeria, J. S. La Pharmacologie Quantique. *Bollettino Chimico Farmaceutico* **1982**, *121*, 619-625.
[3] Gómez-Jeria, J. S. On some problems in quantum pharmacology I. The partition functions. *Int. J. Quant. Chem.* **1983**, *23*, 1969-1972.
[4] Gómez-Jeria, J. S. The use of competitive ligand binding results in QSAR studies. *Il Farmaco; edizione scientifica* **1985**, *40*, 299-302.
[5] Gómez-Jeria, J. S., Morales-Lagos, D., Rodriguez-Gatica, J. I. and Saavedra-Aguilar, J. C. Quantum-chemical study of the relation between electronic structure and pA2 in a series of 5-substituted tryptamines. *Int. J. Quant. Chem.* **1985**, *28*, 421-428.
[6] Gómez-Jeria, J. S., Cassels, B. K. and Saavedra-Aguilar, J. C. A quantum-chemical and experimental study of the hallucinogen (±)-1-(2,5-dimethoxy-4-nitrophenyl)-2-aminopropane (DON). *Euro. J. Med. Chem.* **1987**, *22*, 433-437.
[7] Gómez-Jeria, J. S., "Modeling the Drug-Receptor Interaction in Quantum Pharmacology," in *Molecules in Physics, Chemistry, and Biology*, J. Maruani Ed., vol. 4, pp. 215-231, Springer Netherlands, 1989.
[8] Gómez-Jeria, J. S., Ojeda-Vergara, M. and Donoso-Espinoza, C. Quantum-chemical Structure-Activity Relationships in carbamate insecticides. *Mol. Eng.* **1995**, *5*, 391-401.
[9] Gómez-Jeria, J. S. and Lagos-Arancibia, L. Quantum-chemical structure-affinity studies on kynurenic acid derivatives as Gly/NMDA receptor ligands. *Int. J. Quant. Chem.* **1999**, *71*, 505-511.
[10] Gómez-Jeria, J. S. and Ojeda-Vergara, M. Parametrization of the orientational effects in the drug-receptor interaction. *J. Chil. Chem. Soc.* **2003**, *48*, 119-124.

ISSN 2291-6458 (Print), ISSN 2291-6466 (Online)
Year 2013 | Volume 1 | Issue 3 | Page 215-237

[11] Gómez-Jeria, J. S., Soto-Morales, F., Rivas, J. and Sotomayor, A. A theoretical structure-affinity relationship study of some cannabinoid derivatives. *J. Chil. Chem. Soc.* **2008**, *53*, 1393-1399.

[12] Gómez-Jeria, J. S. A DFT study of the relationships between electronic structure and peripheral benzodiazepine receptor affinity in a group of N,N-dialkyl-2- phenylindol-3-ylglyoxylamides (Erratum in: Journal of the Chilean Chemical Society, 55, 4, IX, 2010). *J. Chil. Chem. Soc.* **2010**, *55*, 381-384.

[13] Barahona-Urbina, C., Nuñez-Gonzalez, S. and Gómez-Jeria, J. S. Model-based quantum-chemical study of the uptake of some polychlorinated pollutant compounds by Zucchini subspecies. *J. Chil. Chem. Soc.* **2012**, *57*, 1497-1503.

[14] Alarcón, D. A., Gatica-Díaz, F. and Gómez-Jeria, J. S. Modeling the relationships between molecular structure and inhibition of virus-induced cytopathic efects. Anti-HIV and anti-H1N1 (Influenza) activities as examples. *J. Chil. Chem. Soc.* **2013**, *58*, 1651-1659.

[15] Gómez-Jeria, J. S. A New Set of Local Reactivity Indices within the Hartree-Fock-Roothaan and Density Functional Theory Frameworks. *Can. Chem. Trans.* **2013**, *1*, 25-55.

[16] Bruna-Larenas, T. and Gómez-Jeria, J. S. A DFT and Semiempirical Model-Based Study of Opioid Receptor Affinity and Selectivity in a Group of Molecules with a Morphine Structural Core. *Int. J. Med. Chem.* **2012**, *2012 Article ID 682495*, 1-16.

[17] Agin, D., Hersh, L. and Holtzman, D. The action of anesthetics on excitable membranes: a quantum-chemical analysis. *Proc. Natl. Acad. Sci. (USA)* **1965**, *53*, 952-958.

[18] Cammarata, A. An Apparent Correlation between the in Vitro Activity of Chloramphenicol Analogs and Electronic Polarizability. *J. Med. Chem.* **1967**, *10*, 525-527.

[19] Cammarata, A. Some electronic factors in drug-receptor interactions. *J. Med. Chem.* **1968**, *11*, 1111-1115.

[20] Cammarata, A. and Stein, R. L. Molecular orbital methods in the study of cholinesterase inhibitors. *J. Med. Chem.* **1968**, *11*, 829-833.

[21] Peradejordi, F., Martin, A. N. and Cammarata, A. Quantum chemical approach to structure-activity relationships of tetracycline antibiotics. *J. Pharm. Sci.* **1971**, *60*, 576-582.

[22] Kim, J., Lee, D., Park, C., So, W., Jo, M., Ok, T., Kwon, J., Kong, S., Jo, S., Kim, Y., Choi, J., Kim, H. C., Ko, Y., Choi, I., Park, Y., Yoon, J., Ju, M. K., Kim, J., Han, S.-J., Kim, T.-H., Cechetto, J., Nam, J., Sommer, P., Liuzzi, M., Lee, J. and No, Z. Discovery of Phenylaminopyridine Derivatives as Novel HIV-1 Non-nucleoside Reverse Transcriptase Inhibitors. *ACS Med. Chem. Lett.* **2012**, *3*, 678-682.

[23] Castro-Castillo, V., Suárez-Rozas, C., Castro-Loiza, N., Theoduloz, C. and Cassels, B. K. Annulation of substituted anthracene-9,10-diones yields promising selectively antiproliferative compounds. *Euro. J. Med. Chem.* **2013**, *62*, 688-692.

[24] Ho, K.-K., Parnell, K. M., Yuan, Y., Xu, Y., Kultgen, S. G., Hamblin, S., Hendrickson, T. F., Luo, B., Foulks, J. M., McCullar, M. V. and Kanner, S. B. Discovery of 4-phenyl-2-phenylaminopyridine based TNIK inhibitors. *Bioorg.Med. Chem. Lett.* **2013**, *23*, 569-573.

[25] Whetsel, K. B. Spectrophotometric Determination of Anthraquinone and Benzanthrone. *Anal.Chem.* **1953**, *25*, 1334-1337.

[26] Rao, A. V. R. and Vaidyanathan, A. The 1H NMR spectrum of benzanthrone. *Spectrochimica Acta Part A: Molecular Spectroscopy* **1981**, *37*, 145-146.

[27] Vaidyanathan, A. The carbon-13 NMR spectra of benzanthrone and its derivatives. *Dyes and Pigments* **1982**, *3*, 243-248.

[28] Srivastava, L. P., Misra, R. B. and Joshi, P. C. Photosensitizing potential of benzanthrone. *Food Chem. Toxicol.* **1990**, *28*, 653-658.

[29] Dabestani, R., Sik, R. H., Motten, A. G. and Chignell, C. F. Spectroscopic studies of cutaneous photosensitizing agents. Xvii. Benzanthrone. *Photochem. Photobiol.* **1992**, *55*, 533-539.

[30] Ribeiro da Silva, M. A. V., Ferrão, M. L., amp, x, sa, C. C. H., Monte, M. J. S., Gonçalves, J. M. and Jiye, F. Standard molar enthalpy of formation, vapour pressures, and standard molar enthalpy of sublimation of benzanthrone. *J. Chem. Thermodyn.* **1999**, *31*, 1067-1075.

ISSN 2291-6458 (Print), ISSN 2291-6466 (Online)
Year 2013 | Volume 1 | Issue 3 | Page 215-237

[31] Gómez-Jeria, J. S., Morales-Lagos, D., Cassels, B. K. and Saavedra-Aguilar, J. C. Electronic structure and serotonin receptor binding affinity of 7-substituted tryptamines QSAR of 7-substituted tryptamines. *Quantitative Structure-Activity Relationships* **1986**, *5*, 153-157.
[32] Gómez-Jeria, J. S. and Ojeda-Vergara, M. Electrostatic medium effects and formal quantum structure-activity relationships in apomorphines interacting with D1 and D2 dopamine receptors. *Int. J. Quant. Chem.* **1997**, *61*, 997-1002.
[33] Tomas, F. and Aulló, J. M. Monoamine oxidase inhibition by β-carbolines: A quantum chemical approach. *J. Pharm. Sci.* **1979**, *68*, 772-776.
[34] Hudson, R. F. and Klopman, G. A general perturbation treatment of chemical reactivity. *Tet. Letters* **1967**, *8*, 1103-1108.
[35] Klopman, G. and Hudson, R. F. Polyelectronic perturbation treatment of chemical reactivity. *Theoret. Chim. Acta* **1967**, *8*, 165-174.
[36] Klopman, G. Chemical reactivity and the concept of charge- and frontier-controlled reactions. *J. Am. Chem. Soc.* **1968**, *90*, 223-234.
[37] Klopman, G. Chemical reactivity and reaction paths; Wiley: New York,, 1974.
[38] Gómez-Jeria, J. S. Elements of Molecular Electronic Pharmacology (in Spanish); Ediciones Sokar: Santiago de Chile, 2013.
[39] Fukui, K. and Fujimoto, H. Frontier orbitals and reaction paths: selected papers of Kenichi Fukui; World Scientific: Singapore; River Edge, N.J., 1997.
[40] Rogers, K. S. and Cammarata, A. A molecular orbital description of the partitioning of aromatic compounds between polar and nonpolar phases. *Biochimica et Biophysica Acta (BBA) - Biomembranes* **1969**, *193*, 22-29.
[41] Rogers, K. S. and Cammarata, A. Superdelocalizability and charge density. A correlation with partition coefficients. *J. Med. Chem.* **1969**, *12*, 692-693.
[42] Cammarata, A. and Rogers, K. S. Electronic representation of the lipophilic parameter π. *J. Med. Chem.* **1971**, *14*, 269-274.
[43] Frisch, M. J., Trucks, G. W., Schlegel, H. B. et al., Gaussian98 Rev. A.11.3, Pittsburgh, PA, USA.2002.
[44] Gómez-Jeria, J. S. An empirical way to correct some drawbacks of Mulliken Population Analysis (Erratum in: Journal of the Chilean Chemical Society, 55, 4, IX, 2010). *J. Chil. Chem. Soc.* **2009**, *54*, 482-485.
[45] Statsoft, Statistica 8.0, 2300 East 14 th St. Tulsa, OK 74104, USA.1984-2007.
.